

## Spin dependent recombination based magnetic resonance spectroscopy of bismuth donor spins in silicon at low magnetic fields

P. A. Mortemousque, T. Sekiguchi, C. Culan, M. P. Vlasenko, R. G. Elliman et al.

Citation: *Appl. Phys. Lett.* **101**, 082409 (2012); doi: 10.1063/1.4747723

View online: <http://dx.doi.org/10.1063/1.4747723>

View Table of Contents: <http://apl.aip.org/resource/1/APPLAB/v101/i8>

Published by the [American Institute of Physics](#).

---

### Related Articles

Electron paramagnetic resonance studies of manganese centers in SrTiO<sub>3</sub>: Non-Kramers Mn<sup>3+</sup> ions and spin-spin coupled Mn<sup>4+</sup> dimers

*J. Appl. Phys.* **111**, 104119 (2012)

Electrical activation and electron spin resonance measurements of implanted bismuth in isotopically enriched silicon-28

*Appl. Phys. Lett.* **100**, 172104 (2012)

Transformation and clustering of defects induced by electron irradiation in barium hollandite ceramics for radioactive cesium storage: Electron paramagnetic resonance study

*J. Appl. Phys.* **111**, 083504 (2012)

Identification of a paramagnetic recombination center in silicon/silicon-dioxide interface

*Appl. Phys. Lett.* **100**, 152107 (2012)

Light-induced electron paramagnetic resonance evidence of charge transfer in electrospun fibers containing conjugated polymer/fullerene and conjugated polymer/fullerene/carbon nanotube blends

*Appl. Phys. Lett.* **100**, 113303 (2012)

---

### Additional information on *Appl. Phys. Lett.*

Journal Homepage: <http://apl.aip.org/>

Journal Information: [http://apl.aip.org/about/about\\_the\\_journal](http://apl.aip.org/about/about_the_journal)

Top downloads: [http://apl.aip.org/features/most\\_downloaded](http://apl.aip.org/features/most_downloaded)

Information for Authors: <http://apl.aip.org/authors>

## ADVERTISEMENT

**AEROTECH**  
nano Motion Technology

Click here for the **FREE**  
nano Motion Technology Catalog

Linear Single-Axis and Dual-Axis Stages

Rotary Stages

Goniometers

Vertical Lift and Z Stages

The advertisement features a blue background with images of various motion stages and goniometers. On the right, there is a vertical image of a catalog cover with the text 'nano Motion Technology' and 'AEROTECH'.

# Spin dependent recombination based magnetic resonance spectroscopy of bismuth donor spins in silicon at low magnetic fields

P. A. Mortemousque,<sup>1</sup> T. Sekiguchi,<sup>1</sup> C. Culan,<sup>1</sup> M. P. Vlasenko,<sup>2</sup> R. G. Elliman,<sup>3</sup>  
L. S. Vlasenko,<sup>2</sup> and K. M. Itoh<sup>1</sup>

<sup>1</sup>*School of Fundamental Science and Technology, Keio University, 3-14-1 Hiyoshi, Kohoku-ku, Yokohama 223-8522, Japan*

<sup>2</sup>*A. F. Ioffe Physico-Technical Institute, Russian Academy of Sciences, 194021, St. Petersburg, Russia*

<sup>3</sup>*Australian National University, Research School of Physics and Engineering, Canberra ACT 0200, Australia*

(Received 12 May 2012; accepted 9 August 2012; published online 22 August 2012)

Low-field (6–110 mT) magnetic resonance of bismuth (Bi) donors in silicon has been observed by monitoring the change in photoconductivity induced by spin dependent recombination. The spectra at various resonance frequencies show signal intensity distributions drastically different from that observed in conventional electron paramagnetic resonance, attributed to different recombination rates for the forty possible combinations of spin states of a pair of a Bi donor and a paramagnetic recombination center. An excellent tunability of Bi excitation energy for the future coupling with superconducting flux qubits at low fields has been demonstrated. © 2012 American Institute of Physics. [<http://dx.doi.org/10.1063/1.4747723>]

Among a variety of qubits investigated for the realization of solid-state quantum computers, superconducting qubits are the leading candidates for quantum processors because of their fast operation capabilities ( $\pi/2$  pulse shorter than 10 ns).<sup>1</sup> However, the shortcoming of their relatively fast decoherence time needs to be overcome by connecting to memory qubits that can store quantum information throughout the course of computation. This requires memory qubits working under low magnetic field, typically below 10 mT for aluminum superconducting qubits,<sup>2</sup> since they cannot operate at higher fields.

In this context, the bismuth (Bi) donor in silicon (Si) has attracted much attention recently. Its large hyperfine interaction  $a/h = 1.4754$  GHz (Ref. 3) and the <sup>209</sup>Bi nuclear spin  $I = 9/2$  give a large zero-field splitting of 7.4 GHz. This splitting is comparable to the typical energy splitting between  $|R\rangle$  and  $|L\rangle$  states of superconducting flux qubits.<sup>1,4</sup> Thus, coupling between a Bi spin qubit and a superconducting flux qubit on Si is in principle possible via a microwave photon through a waveguide. A proposal of such an application<sup>5</sup> has prompted extensive research on the Bi donor spins in Si very recently.<sup>5,6</sup> Starting from the spectroscopic analysis of the electron paramagnetic resonance (EPR),<sup>6,7</sup> the electron spin relaxation time  $T_1$ ,<sup>5,8</sup> decoherence time  $T_2$ ,<sup>5,7,8</sup> and superhyperfine interaction with nearby <sup>29</sup>Si nuclear spins<sup>8</sup> were investigated. Moreover, the coherent transfer between electron and <sup>209</sup>Bi nuclear spins<sup>6</sup> and dynamic nuclear polarization of <sup>209</sup>Bi (Refs. 5 and 9) were achieved. Yet all of these EPR studies were performed at 9 GHz (around 320 mT) and at 240 GHz (around 8.6 T) excitation frequency.

In this paper, we report on low-field (6–110 mT) radio frequency (20–400 MHz) and microwave (8.141 GHz) magnetic resonance, as well as X-band (9 GHz) magnetic resonance, of ion-implanted Bi donors in Si using a highly sensitive, spin dependent recombination based magnetic resonance (SDR-MR) method.<sup>10–13</sup>

The samples were prepared from highly resistive ( $>3000 \Omega \cdot \text{cm}$ ), float-zone (FZ) n-type silicon wafers implanted with Bi ions at room temperature with a total fluence of

$2 \times 10^{12} \text{ cm}^{-2}$ . The implantation energies are 300 and 550 keV with the doses of  $0.7 \times 10^{12}$  and  $1.3 \times 10^{12} \text{ cm}^{-2}$ , respectively. This condition leads to the Bi concentration of about  $1.8 \times 10^{17} \text{ cm}^{-3}$  in the depth of 90 to 150 nm from the surface. The post-implantation annealing was performed at 650 °C for 30 min in an evacuated quartz tube. This annealing condition has been shown to achieve the electrical activation of 80%,<sup>7,14,15</sup> thus yielding about  $4.8 \times 10^{11}$  Bi donors in a  $0.3 \text{ cm}^2$  sample area. The SDR-MR spectra were recorded at 16 K with a commercial continuous wave EPR spectrometer (JEOL JES-RE3X) working at X-band (9 GHz microwave) with a homemade coil for radio frequency (20–400 MHz) and microwave (8.141 GHz) irradiation to induce magnetic resonance at low field (6–110 mT). Continuous illumination with a 100-W halogen lamp generates photocarriers in the sample. Magnetic resonance can enhance the spin-dependent recombination, which decreases the density of photocarriers. Then, the absorption of the microwave electric field by the photocarriers is decreased, leading to an enhancement in the Q-factor of the cavity. Thus, the effect of magnetic resonance can be detected simply as the change in the X-band microwave reflection from the cavity. The second derivative of the reflected intensity with respect to the field modulation was recorded as an SDR signal to reduce the broad cyclotron resonance lines and the background change of the sample resistivity during the magnetic field scan. Note that because of our high power (80 mW) saturating excitation, i.e., making the populations of the ground- and excited-states the same, the conventional EPR absorption signal is suppressed. Such saturation is necessary to flip one of the spins in a pair of Bi and defect to induce SDR as we will discuss later.

The spin system of an isolated Bi donor in static magnetic field  $B_0$  (electron spin  $S = 1/2$  and <sup>209</sup>Bi nuclear spin  $I = 9/2$ ) can be represented by the spin Hamiltonian

$$\mathcal{H} = g\mu_B B_0 S_z - g_n \mu_n B_0 I_z + a\mathbf{S} \cdot \mathbf{I}, \quad (1)$$

where  $\mu_B$  and  $\mu_n$  are the Bohr and nuclear magnetons, and  $g = 2.0003$  (Ref. 3) and  $g_n = 0.914$  (Ref. 5) are Bi electron

and nuclear  $g$ -factors, respectively. The SDR method requires a coupled pair of electron spins.<sup>16–18</sup> In the present study, the partner of the Bi donor electron spin is the electron spin of a deep paramagnetic recombination center (PRC), which is supposed to be created during the implantation process and not completely removed by controlling the annealing conditions.<sup>19</sup> We have attempted to identify the symmetry of the deep PRC by tracing the angular dependence of the EPR peaks. However, the peaks were too broad to draw conclusions.

The X-band (9.076 GHz) SDR-MR spectrum measured without radio frequency excitation is presented in Fig. 1(b). The peaks labeled as Bi-X and PRC indicate ten EPR-“allowed” transitions of the Bi donors and one EPR transition of a PRC, respectively, corresponding to the intersections with the 9.076 GHz excitation in Fig. 1(a). Here, the EPR transition frequencies of the Bi donor (solid curves)<sup>20</sup> were calculated as functions of the static magnetic field  $B_0$  using the spin Hamiltonian in Eq. (1) and that of PRC (dashed curve) was calculated as an isotropic, nuclear spin free, paramagnetic center  $S = 1/2$  and  $g = 2.005(3)$ . The same notation as in Ref. 20 for labeling Bi eigenstates is used; the labels 1 to 20 in increasing order of energy.

In addition, two lines labeled as CR1 (186 mT) and CR2 (259 mT) arise due not to the resonance with the 9.076 GHz microwave but to cross relaxation (CR) between particular Bi donor transitions and the PRC transitions, in a way very similar to the cross relaxation between phosphorus donors and SL1 centers in Si observed by electrically detected magnetic resonance.<sup>21</sup> This assignment of CR1 and CR2 is further justified in Fig. 2. Even with the decrease in the microwave excitation frequency, the position of these lines remains the same, whereas the Bi EPR line positions shift to

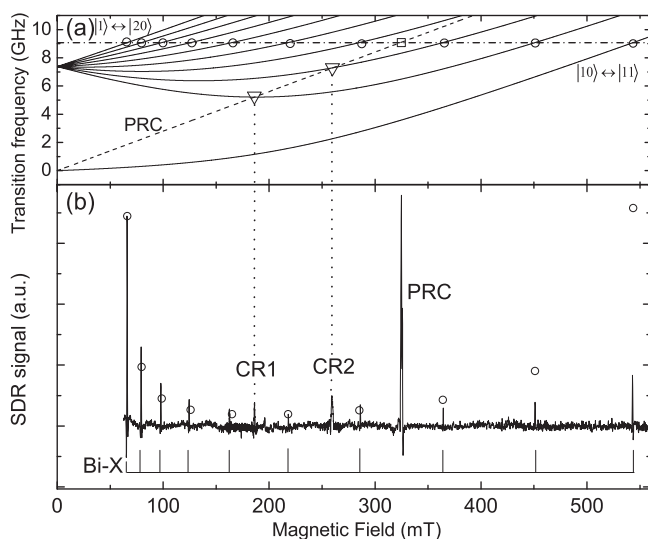


FIG. 1. (a) Calculated EPR transition frequencies of Bi donors (solid curves) and deep PRC (dashed line) with 9.076 GHz microwave excitation frequency (dotted-dashed line). The intersections of the PRC transition energy with bismuth donor transitions (open triangles) and with the 9.076 GHz microwave (open square) are also shown. (b) An SDR-MR spectrum of Bi donors in Si recorded at 16 K under illumination. The 9.076 GHz microwave is used both to induce Bi EPR transition and to probe the change in the sample photoconductivity. CR1 and CR2 are the cross relaxation signals between Bi and PRC. The open circles in (b) indicate simulated intensities using the SDR model described in the text with the parameter value of  $R_p/R_{ap} = 0.01$ .

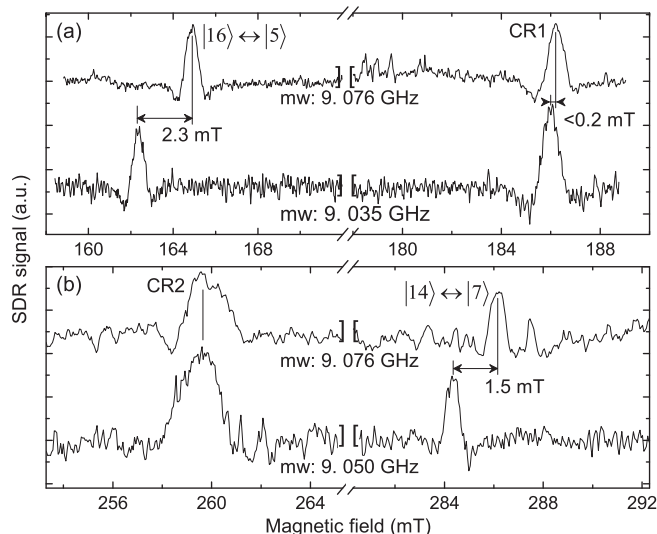


FIG. 2. Cross relaxation lines CR1 (a) and CR2 (b) together with SDR-MR Bi lines detected at different microwave frequencies. The Bi EPR lines labeled as  $|16\rangle \leftrightarrow |5\rangle$  in (a) and  $|14\rangle \leftrightarrow |7\rangle$  in (b) shift with the resonant frequency whereas the lines CR1 and CR2 do not. Additionally, the CR1 line is narrower than CR2 because, as shown in Fig. 1(a), the difference in the field-derivative of the transition frequency between the paramagnetic recombination center and resonant Bi transition is larger.

lower fields. This proves the presence of coupling between the Bi donor and PRC electron spins, which is requisite for the SDR detection method.

We should emphasize that even at the same X-band resonance of the Bi donor, the observed SDR-MR line intensity distribution is clearly different from that observed in the conventional EPR spectra.<sup>5,6,8,20</sup> The intensity differs for the ten different transitions in the present SDR-MR, whereas it is practically the same in conventional EPR, reflecting simply the thermal equilibrium population difference between the involved levels. Furthermore, the observed line-dependence of the SDR-MR intensity is distinctively stronger than the line dependence in the EPR transition.<sup>20</sup>

Figure 3(a) shows the SDR-MR spectra probed by the same X-band microwave but with additional radio frequency excitation of 50 or 200 MHz. A simulation of the 200 MHz SDR-MR spectrum based on the SDR model that will be introduced later is also shown. Figure 3(b) shows the observed SDR-MR line positions (solid circles) for radio frequency excitation ranging from 20 to 400 MHz together with the calculated magnetic resonance transition frequencies for the Bi donor (solid curves). All of these simulated Bi magnetic resonance transitions are the  $^{209}\text{Bi}$  NMR transitions in the high field limit. While the number of calculated Bi NMR lines in Fig. 3(b) appears ten, all but the lowest- and highest-field lines are nearly degenerate doublets, i.e., each is composed of two lines separated by exactly twice the nuclear Zeeman splitting energy. Therefore, among the eighteen EPR transitions of the Bi donor excited by these radio frequencies, we observed clearly the two non-degenerate lines labeled as Bi-RF in Fig. 3. The remaining eight doublets are too weak to be observed with the current experimental conditions.

As mentioned above, considering only the EPR transition probabilities<sup>20</sup> cannot describe the intensity of SDR-MR. In the following, we shall present a model, based on the SDR

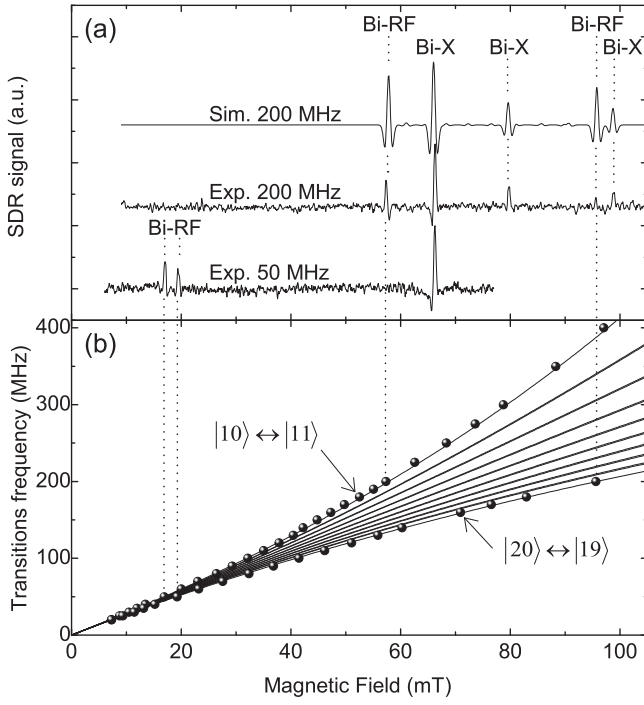


FIG. 3. (a) Low-field SDR-MR spectra with 50 and 200 MHz resonance frequencies together with simulation of the 200 MHz spectrum. The transitions by the radio frequencies and X-band 9.076 GHz microwave are labeled as Bi-RF and Bi-X, respectively. The line intensities are simulated using the same model and parameters as for Fig. 1(b). (b) The Bi-RF line positions observed at various resonant frequencies (solid circles) together with calculated resonant fields (solid lines).

model developed in Refs. 22–24, to simulate the SDR-MR spectra that are shown in Figs. 1(b) and 3(a). The SDR signal intensity, measured by probing the microwave intensity reflected by the cavity, is linear to the sample photoconductivity  $\sigma$ . Its change by magnetic resonance through SDR process can be written as

$$\Delta\sigma \propto -\sum_{i,\mu} R_{i,\mu} [N_{i,\mu}(w \rightarrow \infty) - N_{i,\mu}(w = 0)], \quad (2)$$

where the subscripts  $i$  and  $\mu$  denote the Bi donor and PRC spin states, respectively.  $R_{i,\mu}$  and  $N_{i,\mu}$  are the recombination rate and population of the specified pair. Here, the square bracket represents the change in the population from off-resonance ( $w = 0$ ) to saturated magnetic resonance ( $w \rightarrow \infty$ ) conditions where  $w$  is the excitation power. Equation (2) is valid when the recombination rates can be assumed dominant over the pair generation and dissociation rates as well as the spin-lattice relaxation and spin decoherence rates. Furthermore, if only one transition between two Bi states  $i$  and  $j$  is selectively excited, the change in photoconductivity becomes

$$\Delta\sigma(i,j) \approx -\sum_{\mu} [R_{i,\mu} N_{i,\mu}(\infty) + R_{j,\mu} N_{j,\mu}(\infty) - (R_{i,\mu} N_{i,\mu}(0) + R_{j,\mu} N_{j,\mu}(0))]. \quad (3)$$

Using the rate equations described in Ref. 17, Eq. (3) simplifies to

$$\Delta\sigma(i,j) \approx -\sum_{\mu} \left[ \frac{4}{R_{i,\mu} + R_{j,\mu}} - \left( \frac{1}{R_{i,\mu}} + \frac{1}{R_{j,\mu}} \right) \right]. \quad (4)$$

The first term of Eq. (4) corresponds to the number of recombining pairs when the resonance is saturated, whereas the second and third terms are the off-resonance terms. Thus, a large change in SDR signal should be obtained when either  $R_{i,\mu}$  or  $R_{j,\mu}$  is much smaller than the other. Finally, to evaluate the recombination rates  $R_{i,\mu}$  and  $R_{j,\mu}$ , the product state of the Bi donor and the PRC is considered

$$|i\rangle|\mu\rangle = (\cos\phi_i(B_0)|1/2, M - 1/2\rangle + \sin\phi_i(B_0)|-1/2, M + 1/2\rangle)|\mu\rangle. \quad (5)$$

In the right-hand side, the Bi state ( $i \in [1, 20]$ ) is represented by the product of the electron ( $m_s = \pm 1/2$ ) and nuclear spin ( $-9/2 \leq m_l \leq 9/2$ ) states with the total spin  $z$ -component of  $-5 \leq M \leq 5$  is represented on the basis of the electron ( $m_s$ ) and nuclear ( $m_l$ ) spin  $z$ -component eigenstates.<sup>25</sup> Note that there are two different Bi eigenstates for one particular  $M$ , except for  $M = \pm 5$ . The mixing angle  $\phi_i(B_0)$  depends on the Bi state and is a function of the parameters in the Hamiltonian, Eq. (1), as explicitly described in Ref. 20. Depending on the state of PRC ( $\mu = \pm 1/2$ , denoted by  $\mu = \uparrow, \downarrow$ ), each term in Eq. (5) gives contribution to the recombination rate in terms of spin parallel ( $R_p$ ) or anti-parallel ( $R_{ap}$ ) pair

$$R_{i,\uparrow}(B_0) = R_p \cos^2\phi_i(B_0) + R_{ap} \sin^2\phi_i(B_0), \quad (6)$$

$$R_{i,\downarrow}(B_0) = R_p \sin^2\phi_i(B_0) + R_{ap} \cos^2\phi_i(B_0). \quad (7)$$

Then, only the recombination associated with the pure states,  $i = 10$  ( $M = -5$ ) and  $i = 20$  ( $M = +5$ ), has single components that are strictly parallel or anti-parallel, while the other states have a mixture of the two components. This, in combination with Eq. (4), is the reason why the highest- and lowest-field lines, which involve the Bi state  $|10\rangle$  or  $|20\rangle$ , are stronger than the other lines at X-band resonance and exclusively strongest at the radio frequency resonance. We used this model to perform the simulation of the X-band spectrum in Fig. 1(b) and the 200 MHz spectrum in Fig. 3(a). The ratio  $R_p/R_{ap} = 0.01$  has led to good agreement with the experiments and is comparable to the recently reported value  $15 \mu\text{s} / 2 \text{ms} = 0.0075$  for the phosphorus donor in Si.<sup>26</sup> Note that, for the X-band spectrum, we also take into account that an EPR transition line that is “forbidden” in the high-field limit overlaps with each EPR-“allowed” one except for the highest- and lowest-field lines that involve one pure state.<sup>20</sup>

Finally, we shall demonstrate the tunability of such “pure-state” transitions to the energy comparable to the superconducting qubits. As shown in Fig. 4(a), an additional 8.141 GHz microwave excitation in the same SDR method allows for successful excitation and detection of the EPR transition between Bi  $|1\rangle$  and  $|20\rangle$  levels at low field ( $B_0 = 30 \text{mT}$ ). Although it is preferred to achieve  $B_0 < 10 \text{mT}$  for the coupling with the superconducting qubit, Fig. 4 shows clearly the flexibility to tune the energy difference between up and down states of the Bi electron spin. It is also possible to tune the superconducting flux qubit to match the energy between  $|R\rangle$  and  $|L\rangle$  states with the Bi transition frequency separating  $|1\rangle$  and  $|20\rangle$  states. The coupling strength between the flux qubit and Bi is expected in the range of 1–100 kHz.<sup>4</sup> Figure 4(b) shows a result of a similar

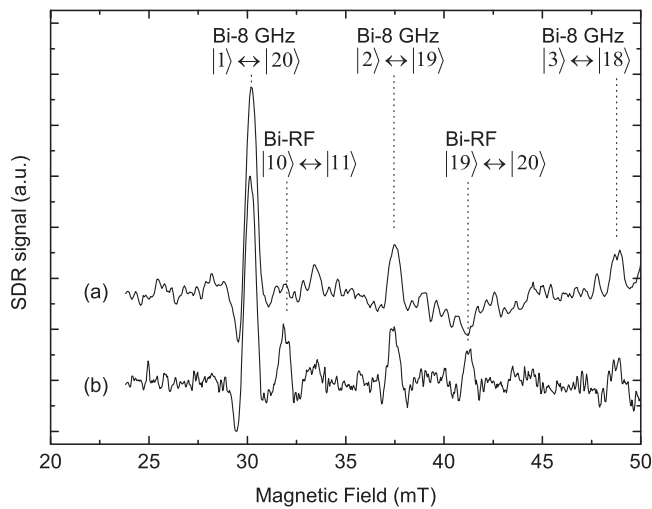


FIG. 4. Low-field SDR-MR spectra probed by the 9.076 GHz X-band reflection (a) with a single 8.141 GHz excitation frequency and (b) with the same 8.141 GHz excitation plus an additional 100 MHz radio frequency. The lines resonant with the 8.141 GHz microwave and the 100 MHz radio frequency are labeled as Bi-8 GHz and Bi-RF, respectively.

experiment but with two excitation frequencies generated by two coils perpendicular to each other. The second coil was used to irradiate 100-MHz excitation frequency. The Bi-RF and Bi-8 GHz resonance lines are observed together. Hence, this experimental setup allows us to perform SDR-MR with two arbitrary excitation frequencies.

In summary, we have obtained the electron paramagnetic resonance spectra of a small number ( $5 \times 10^{11}$ ) of Bi donors in Si at low magnetic field (6–110 mT). The detection was based on the measurement of the sample photoconductivity which changed significantly at the time of resonance due to specific spin-dependent-recombination phenomena. The spin-dependent-recombination process takes place via coupling of the electron spins between Bi donors and nearby paramagnetic recombination centers. The relative intensity of each resonance line has been described well by a spin-dependent-recombination model based on the mixing of Bi donor electron and nuclear spins.

This work was supported in part by Grant-in-Aid for Scientific Research and Project for Developing Innovation Systems by MEXT, FIRST, and JST-EPSRC/SIC (EP/H025952/1).

- <sup>1</sup>I. Chiorescu, Y. Nakamura, C. J. P. M. Harmans, and J. E. Mooij, *Science* **299**, 1869 (2003).
- <sup>2</sup>J. F. Cochran and D. E. Matpothier, *Phys. Rev.* **111**, 132 (1958).
- <sup>3</sup>G. Feher, *Phys. Rev.* **114**, 1219 (1959).
- <sup>4</sup>X. Zhu, S. Saito, A. Kemp, K. Kakuyanago, S. Karimoto, H. Nakano, W. J. Munro, Y. Tokura, M. S. Everitt, K. Nemoto, M. Kasu, N. Mizuochi, and K. Semba, *Nature (London)* **478**, 221 (2011).
- <sup>5</sup>G. W. Morley, M. Warner, A. M. Stoneham, P. T. Greenland, J. van Tol, C. W. M. Kay, and G. Aeppli, *Nature Mater.* **9**, 725 (2010).
- <sup>6</sup>R. E. George, W. Witzel, H. Riemann, N. V. Abrosimov, N. Nötzel, M. L. W. Thewalt, and J. J. L. Morton, *Phys. Rev. Lett.* **105**, 067601 (2010).
- <sup>7</sup>C. D. Weis, C. C. Lo, V. Lang, A. M. Tyryshkin, R. E. George, K. M. Yu, J. Bokor, S. A. Lyon, J. J. L. Morton, and T. Schenkel, *Appl. Phys. Lett.* **100**, 172104 (2012).
- <sup>8</sup>M. Belli, M. Fanciulli, and N. Abrosimov, *Phys. Rev. B* **83**, 235204 (2011).
- <sup>9</sup>T. Sekiguchi, M. Steger, K. Saedi, M. L. W. Thewalt, H. Riemann, N. V. Abrosimov, and N. Nötzel, *Phys. Rev. Lett.* **104**, 137402 (2010).
- <sup>10</sup>R. L. Vranich, B. Henderson, and M. Pepper, *Appl. Phys. Lett.* **52**, 1161 (1988).
- <sup>11</sup>L. S. Vlasenko, M. P. Vlasenko, T. Gregorkiewicz, and C. A. J. Ammerlaan, *Phys. Rev. B* **52**, 1144 (1995).
- <sup>12</sup>R. Laiho, L. S. Vlasenko, and M. P. Vlasenko, *Mater. Sci. Forum* **196**, 517 (1995).
- <sup>13</sup>L. S. Vlasenko and M. P. Vlasenko, *Mater. Sci. Forum* **196**, 1537 (1995).
- <sup>14</sup>J. P. Souza and P. F. P. Fichtner, *J. Appl. Phys.* **74**, 119 (1993).
- <sup>15</sup>R. Baron, G. A. Shifrin, and O. J. Marsh, *J. Appl. Phys.* **40**, 3702 (1969).
- <sup>16</sup>D. Kaplan, I. Solomon, and N. F. Mott, *J. Phys. (France) Lett.* **39**, 51 (1978).
- <sup>17</sup>R. T. Cox, D. Block, A. Herve, R. Picard, C. Santier, and R. Heibig, *Solid State Commun.* **25**, 77 (1978).
- <sup>18</sup>H. Morishita, L. S. Vlasenko, H. Tanaka, K. Semba, K. Sawano, Y. Shiraki, M. Eto, and K. M. Itoh, *Phys. Rev. B* **80**, 205206 (2009).
- <sup>19</sup>V. Miksic, B. Pivac, B. Rakvin, H. Zorc, F. Corni, R. Tonini, and G. Ottaviani, *Nucl. Instrum. Methods Phys. Res. B* **186**, 36 (2002).
- <sup>20</sup>M. Mohammady, G. Morley, and T. Monteiro, *Phys. Rev. Lett.* **105**, 067602 (2010).
- <sup>21</sup>W. Akhtar, H. Morishita, K. Sawano, Y. Shiraki, L. S. Vlasenko, and K. M. Itoh, *Phys. Rev. B* **84**, 045204 (2011).
- <sup>22</sup>C. Boehme and K. Lips, *Appl. Phys. Lett.* **79**, 4363 (2001).
- <sup>23</sup>C. Boehme and K. Lips, *Phys. Rev. B* **68**, 245105 (2003).
- <sup>24</sup>C. Boehme and K. Lips, *Charge Transport in Disordered Solids*, edited by S. Baranovski (Wiley, 2006), pp. 179–219.
- <sup>25</sup>A. Abragam and B. Bleaney, *Electron Paramagnetic Resonance of Transition Ions* (Oxford University Press, Oxford, UK, 1970).
- <sup>26</sup>L. Dreher, F. Hoehne, M. Stutzmann, and M. S. Brandt, *Phys. Rev. Lett.* **108**, 027602 (2012).